Journal of Alloys and Compounds 636 (2015) 357–362

Contents lists available at ScienceDirect

Journal of Alloys and Compounds

journal homepage: www.elsevier.com/locate/jalcom

Letter

Flower-like NiO hierarchical microspheres self-assembled with nanosheets: Surfactant-free solvothermal synthesis and their gas sensing properties

Xiaoguang San [a], Guosheng Wang [a], Bing Liang [b], Jiao Ma [a], Dan Meng [a,*], Yanbai Shen [c,*]

[a] College of Chemical Engineering, Shenyang University of Chemical Technology, Shenyang 110142, China
[b] College of Materials Science and Engineering, Shenyang University of Chemical Technology, Shenyang 110142, China
[c] College of Resources and Civil Engineering, Northeastern University, Shenyang 110819, China

A R T I C L E I N F O

Article history:
Received 12 January 2015
Received in revised form 24 February 2015
Accepted 25 February 2015
Available online 3 March 2015

Keywords:
Nickel oxide
Hierarchical architecture
Solvothermal
Sensing property

A B S T R A C T

Flower-like NiO hierarchical microspheres self-assembled with thin nanosheets were successfully synthesized by surfactant-free solvothermal method. The obtained product was characterized by means of X-ray diffraction, scanning electron microscopy, and ultraviolet–visible spectroscopy. The results showed that flower-like NiO hierarchical microspheres with a cubic structure were assembled by a number of thin nanosheets with a thickness of about 10 nm. Reaction time was an important parameter for the synthesis of perfect flower-like microspheres. The band gap energy of NiO hierarchical microspheres was estimated to be 3.68 eV. The gas sensing properties showed that the sensor exhibited the highest sensitivity of 3.2 for 100 ppm ethanol at an operating temperature of 250 °C. The reversible response to ethanol at various operating temperatures and gas concentrations and good selectivity were obtained, implying a potential application for the fabrication of high performance ethanol sensors.

1. Introduction

In recent years, the novel three-dimensional (3D) hierarchical architectures assembled by low dimensional nano-building blocks such as nanoparticles, nanowires, and nanosheets, have attracted considerable attention due to its unique properties and wide practical application [1,2]. Because of their high specific surface areas and excellent structural stability, as well as their outstanding transportation properties, these kinds of nanostructures have exhibited superior performance for catalysis, solar cell, sensor, etc [3–7]. For example, Ko et al. [3] reported that tree-like hierarchical ZnO nanostructures assembled by ZnO nanowires demonstrated potential application in dye-sensitized solar cell. Li et al. [5] reported that hierarchical meso-macroporous SnO_2 exhibited higher gas response and shorter response/recovery times in detecting indoor air pollutants. Up to now, various routes have been employed successfully to assemble building blocks into 3D hierarchical architectures [3–7]. The method of hydrothermal/solvethermal is widely used to synthesize hierarchical architectures. However, some surfactants or templates are usually introduced, which causes contamination in the products and subsequently affects various semiconductor device applications. Thus, a facile surfactant- or template-free method for producing hierarchical architecture materials is great significance from the view of both scientific research and practical application.

Nickel oxide (NiO), a p-type metal oxide semiconductor, has been widely used for different fields, such as catalysts [4,8], supercapacitors [9], lithium ion batteries [10], electrochromic devices [11] and so on. Moreover, NiO is one of the promising materials used as gas sensors due to its good sensing properties [12,13]. From the viewpoint of gas sensor, hierarchical architectures with high specific surface areas and porous structures are advantageous for improving the gas sensing performance [14]. Recently, a variety of metal oxide semiconductors such as SnO_2 [5,15], WO_3 [16], and ZnO [17] with hierarchical structures have been synthesized and showed good sensing properties to the detected gases. However, there is little report about gas sensing properties for NiO hierarchical architectures, though which has been widely investigated in many other application fields [4,18,19]. In this study, we report on the synthesis of flower-like NiO hierarchical microspheres composed of thin nanosheets through solvethermal process without using any surfactant. Ethanol gas sensing properties of these flower-like microspheres were investigated.

* Corresponding authors.
E-mail addresses: mengdan0610@hotmail.com (D. Meng), shenyanbai@mail.neu.edu.cn (Y. Shen).

http://dx.doi.org/10.1016/j.jallcom.2015.02.191
0925-8388/

2. Experimental

Flower-like NiO hierarchical microspheres were synthesized by the surfactant-free solvothermal method. In a typical procedure, 0.466 g of nickel nitrate hexahydrate ($Ni(NO_3)_2{\cdot}6H_2O$) was dissolved in 40 mL N, N dimethyl formamide (DMF) under magnetic stirring at room temperature to get a clear solution. Then the solution was transferred into a 50 ml Teflon-lined stainless autoclave, which was sealed and maintained at 180 °C for 12 h and subsequently cooled down to room temperature naturally. A green-blue precipitate was obtained, which was washed with distilled water and ethanol for several times, and dried in vacuum at 60 °C for 4 h. Finally, the black product was obtained through annealing at 400 °C for 4 h in air. The obtained product was characterized using an X-ray diffractometer (XRD, PANalytical X'Pert Pro), a field emission scanning electron microscope (FESEM, ZEISS Ultra Plus) equipped with energy dispersive X-ray spectroscopy (EDS), and ultraviolet–visible spectrometer (UV–Vis, UV-2550, Shimadzu).

3. Results and discussion

3.1. Structure characterizations

SEM images of the as-synthesized and annealed products are shown in Fig. 1. Fig. 1(a) and (b) indicate that the products before annealing are composed of the flower-like microspheres with a diameter ranging from 1 to 3 μm. These flower-like microspheres are constructed by many thin nanosheets with smooth surface and about 10 nm in thickness, which are densely packed and formed a multilayered structure. It is interesting that the follower-like microspheres are successfully sustained after annealing at 400 °C for 4 h (Fig. 1(c) and (d)). In addition, it should be noted that the diameter of these flower-like microspheres does not change after annealing process.

The XRD pattern observed for the as-synthesized and annealed products are shown in Fig. 2(a). All the diffraction peaks of the as-synthesized products could be indexed to single phase α-$Ni(OH)_2$ with a hexagonal crystalline structure (JCPDS card No. 22-0444). No impurity peaks are found in the XRD pattern, suggesting a high purity of the as-synthesized α-$Ni(OH)_2$. The wide peaks and weak peak intensities imply that the crystalline structure of the as-synthesized products is not good. After annealing at 400 °C for 4 h, five main peaks corresponding to the crystallographic planes of (1 1 1), (2 0 0), (2 2 0), (3 1 1), and (2 2 2) are observed (Fig. 2(a)), which characterize a cubic structure of the NiO (JCPDS card No. 47-1049). The sharp diffraction peaks suggest that the high crystallinity of NiO is obtained. Especially, no diffraction peaks of α-$Ni(OH)_2$ are observed, indicating that the α-$Ni(OH)_2$ was completely transformed to NiO after annealing. To demonstrate the chemical composition of the flower-like microspheres, EDS analysis of the annealed product was performed and the EDS spectrum is illustrated in Fig. 2(b). It can be seen that only oxygen and nickel elements exist in the microspheres with O/Ni molar ratio of nearly 1.

It is well known that reaction time has a great effect on the structure and morphology of the product in solvothermal method [20–22]. SEM images of the as-synthesized products at different reaction times are shown in Fig. 3. No precipitation is obtained when the reaction time is less than 3 h. At the reaction time of 4 h, many irregular shapes consist of sheets, rods, and cubics are obtained as shown in Fig. 3(a). Some of them aggregate with each other and form the flower-like microspheres. After increasing reaction time to 8 h, as shown in Fig. 3(b), many incompact aggregations with flower-like structures are obtained, which are assembled by a few nanosheets. At the reaction time of 12 h, the perfect flower-like microspheres consisted of abundant thin nanosheets are found (Fig. 1(a) and (b)). The products remain the flower-like structures at 18 h and show stone-like structures at 24 h, while the diameter of these flower-like microspheres increases from 2 to 8 μm (Fig. 3(c) and (d)). Such results reveal that the reaction time is the main factor to form nanosheet based NiO microspheres. In the present work, hydrate $Ni(NO_3)_2{\cdot}6H_2O$ was used as Ni^{2+} ion source. Thus, the water molecules existed in $Ni(NO_3)_2{\cdot}6H_2O$ are free after it dissolves into the DMF solvent. In the solvothermal process, the water molecules provide OH^- ions for the formation of $Ni(OH)_2$ nuclei, which subsequently grows to nanosheets. As the reaction time increases, in order to reduce the surface energy, the thin nanosheets gradually self-oriented and assembled to flower-like hierarchical $Ni(OH)_2$ structures [21]. Ostwald ripening process maybe plays an important role in this procedure [20–22]. The size increase can significantly decrease the surface free energy and enhance the stability energy of nanosheets, thus leading to the size increase of flower-like microspheres and formation of stone-like structures as extending reaction time. After annealing at 400 °C, the $Ni(OH)_2$ precursors are decomposed and NiO flower-like microspheres are formed.

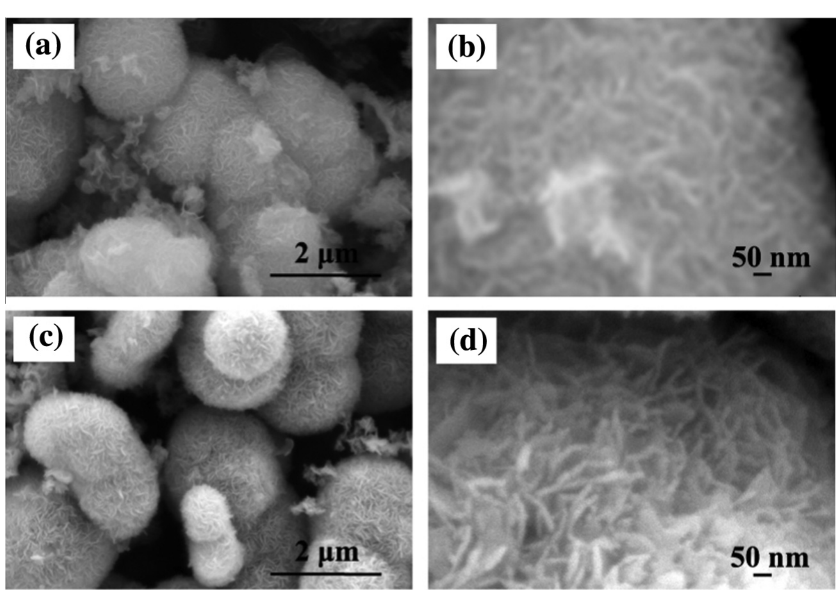

Fig. 1. SEM images of the as-synthesized and annealed products. (a) and (b) as-synthesized products. (c) and (d) products annealed at 400 °C.

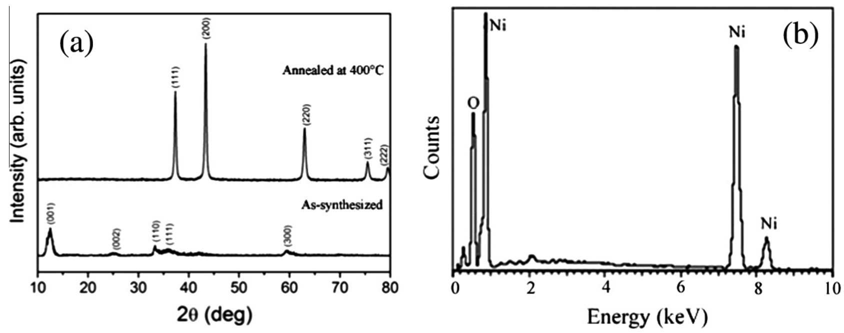

Fig. 2. (a) XRD patterns of the as-synthesized and annealed products. (b) EDS pattern of the product annealed at 400 °C.

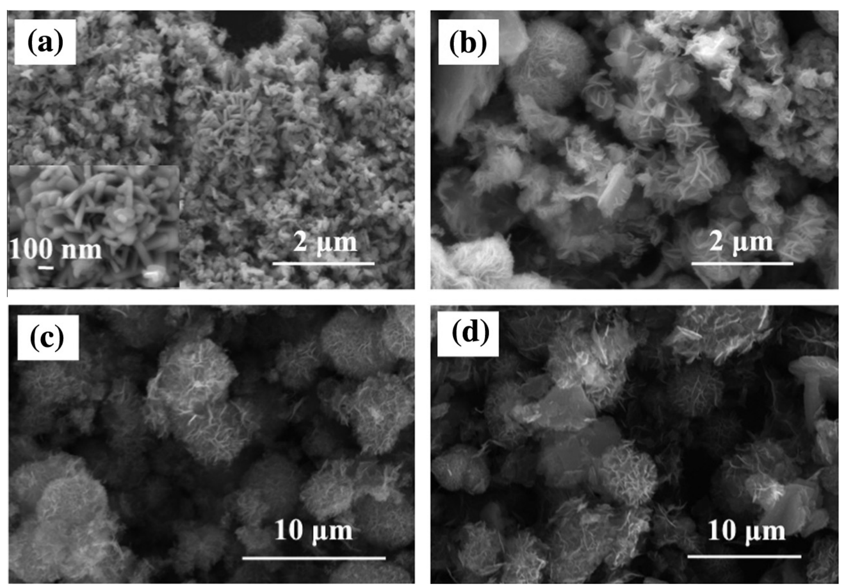

Fig. 3. SEM images of the as-synthesized products at different reaction times. (a) 4 h. (b) 8 h. (c) 18 h. (d) 24 h.

UV–Vis absorption spectrum of the NiO hierarchical microspheres annealed at 400 °C is shown in Fig. 4. The absorption in the UV region can be observed, which may be attributed to the band gap absorption in NiO [23]. The band gap energy (E_g) is usually calculated by the optical absorption spectrum using the following equation $(\alpha h\nu)^n = B(h\nu - E_g)$, where α is absorption coefficient, $h\nu$ is the photo energy, B is a constant relative to the material and n is either 2 for direct transition or 1/2 for an indirect transition [24]. NiO is generally a direct transition semiconductor [25]. Hence, the direct band gap can be obtained by extrapolating the linear portion of the $(\alpha h\nu)^2$ versus $h\nu$ curve to zero, as shown in inset Fig. 4. The derived band gap energy of the NiO hierarchical microspheres was estimated to be 3.68 eV, which is lower than that of the bulk NiO (~3.9 eV) [26]. This is due to the chemical defects or vacancies present in the intergranular regions, forming a new energy level to reduce the band gap energy [25,27].

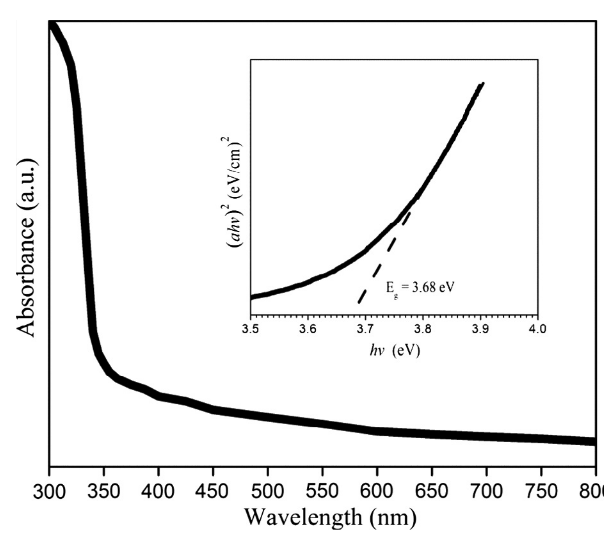

Fig. 4. UV–Vis absorption spectrum of the NiO hierarchical microspheres. The inset is the $(\alpha h\nu)^2 - h\nu$ curve.

3.2. Gas sensing properties

The unique hierarchical microspheres with many petals, pores, and intervals are very good candidates for gas sensors [14]. In this study, gas sensor was fabricated by coating the annealed product onto an alumina ceramic tube attached with a pair of Au electrodes and four Pt wires. A Ni–Cr alloy coil was inserted through the tube to control the operating temperature of the sensor. The gas sensing properties were performed on a static system with the constant loop voltage of 5 V. A diagram of NiO hierarchical microspheres based gas sensor device and measurement electric circuit are shown in Fig. 5(a). The sensitivity is defined as R_g/R_a, where R_a and R_g are the resistances in air and in the tested gas, respectively.

The sensitivities of the sensors made of flower-like NiO hierarchical microspheres upon exposure to 100 ppm ethanol gas are shown in Fig. 5(b) as a function of the operating temperature. The sensor has an optimal operating temperature, at which the sensor exhibits the highest sensitivity to ethanol gas. The highest sensitivity is estimated to be 3.2 at 250 °C. The gas response and recovery behavior of the sensor measured at different operating temperatures to 100 ppm ethanol is shown in Fig. 5(c). The resistance quickly increases when the sensor is exposed to ethanol gas. The response times (the time for the resistance increases to 90% of the maximum) are less than 1 min at all operating temperatures. It is also noted that the resistance can recover to the initial values after removing ethanol gas, indicating a good reversibility. Fig. 5(d) shows the temporal responses of the sensor upon exposure to different concentration ethanol gases (50–1000 ppm) at 250 °C. As the gas concentration increases, the response is enhanced and the resistance can recover to the initial value after removal of ethanol, exhibiting a good reversibility. Gas responses to 100 ppm different volatile organic compound gases were also measured at 250 °C as shown in Fig. 5(e). The result shows that the sensitivity to ethanol is higher than that to other gases, implying that selective detecting of ethanol is possible.

It is well known that NiO belongs to p-type semiconductor, which is a surface controlled process, that is, the sensitivity greatly depends on the adsorption and desorption of gas molecules [12]. A possible sensing mechanism is proposed in Fig. 6. The oxygen molecules from the ambient atmosphere are initially adsorbed on the surface of NiO in the form of O_2^-, O^-, and O^{2-}, depending on the ambient temperature [28,29]. The high coverage with adsorbed oxygen causes the accumulation of holes near the surface of NiO, and thus showing a relatively low resistance state in air ambient. When NiO hierarchical microspheres are exposed to a reducing gas such as ethanol, these gas molecules could react with surface oxygen species by $C_2H_5OH(gas) + 6O^-(ads) \rightarrow 2CO_2 + 3H_2O + 6e^-$ [30]. This process releases the electrons back to NiO, which induces a decrease of the hole concentration by electron-hole recombination, leading to an increase in the resistance. That is the characteristic of p-type semiconductor [31]. The flower-like NiO structure may be beneficial to enhance the probability to absorb target gases and provide an effective gas diffusion path via well-aligned porous architectures, therefore, resulting in good sensing properties [14]. Here, it should be noted that a high response to reducing gas is relatively difficult to accomplish in p-type semiconductors, even with the considerably large surface changes due to the conduction

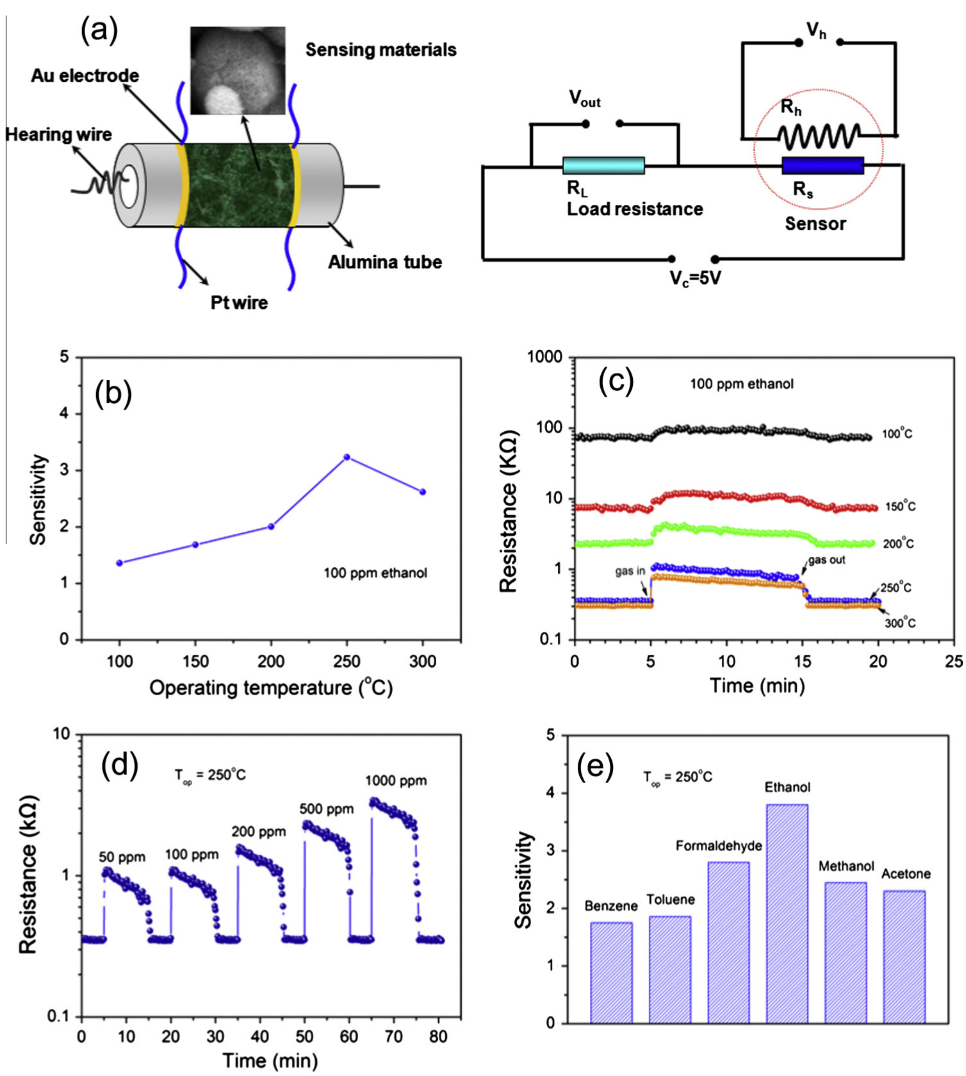

Fig. 5. (a) Schematic illustration of the gas sensor and measurement electric circuit. (b) Sensitivity and (c) temporal responses upon exposure to 100 ppm ethanol gas at different operating temperatures. (d) Temporal responses to ethanol gases with various concentrations at 250 °C. (e) Selectivity to different gases with concentration of 100 ppm.

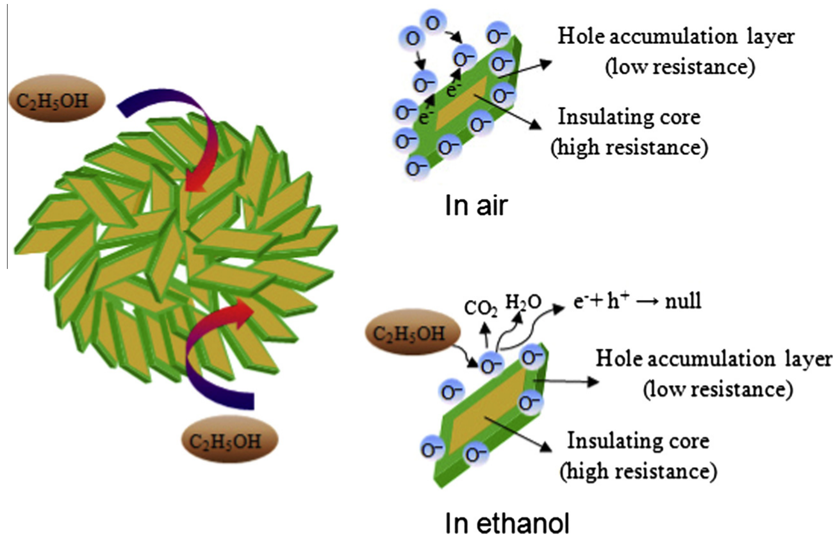

Fig. 6. Schematic illustration of gas sensing mechanism.

mechanism [32]. A further investigation on the sensing properties of flower-like NiO microsphere is still required.

4. Conclusions

High-performance flower-like NiO hierarchical microspheres assembled with thin nanosheets were successfully synthesized by surfactant-free solvethermal method. The structure characteristics and ethanol sensing properties of NiO hierarchical microspheres were investigated. The results showed that NiO hierarchical microspheres with a cubic structure were assembled by a number of thin nanosheets with a thickness of about 10 nm. The band gap energy of NiO hierarchical microspheres was estimated to be 3.68 eV. Ethanol sensing measurements indicated that NiO hierarchical microspheres exhibited the highest sensitivity of 3.2–100 ppm ethanol at an operating temperature of 250 °C and reversible response to ethanol at various operating temperatures and concentrations. The results indicate a potential application for the fabrication of high-performance ethanol sensors.

Acknowledgements

The authors are grateful for the support of the National Natural Science Foundation of China (61403263, 51422402) and Liaoning Educational Department Foundation (L2014167).

References

[1] V. Polshettiwar, B. Baruwati, R.S. Varma, Self-assembly of metal oxides into three-dimensional nanostructures: synthesis and application in catalysis, ACS Nano 3 (2009) 728–736.
[2] Y.F. Sun, S.B. Liu, F.L. Meng, J.Y. Liu, Z. Jin, L.T. Kong, J.H. Liu, Metal oxide nanostructures and their gas sensing properties, Sensors 12 (2012) 2610–2631.
[3] S.H. Ko, D. Lee, H.W. Kang, K.H. Nam, J.Y. Yeo, S.J. Hong, C.P. Grigoropoulos, H.J. Sung, Nanoforest of hydrothermally grown hierarchical ZnO nanowires for a high efficiency dye-densitized solar cell, Nano Lett. 11 (2011) 666–671.
[4] B. Zhao, X.K. Ke, J.H. Bao, C.L. Wang, L. Dong, Y.W. Chen, H.L. Chen, Synthesis of flower-like NiO and effects of morphology on its catalytic properties, J. Phys. Chem. C 113 (2009) 14440–14447.
[5] H.H. Li, F.L. Meng, J.Y. Liu, Y.F. Sun, Z. Jin, L.T. Kong, Y.J. Hu, J.H. Liu, Synthesis and gas sensing properties of hierarchical meso-macroporous SnO_2 for detection of indoor air pollutants, Sens. Actuators B 519 (2012) 166–167.
[6] L.L. Yang, Q.F. Han, J. Zhao, J.W. Zhu, X. Wang, W.H. Ma, Synthesis of Bi_2O_3 architectures in DMF–H_2O solution by precipitation method and their photocatalytic activity, J. Alloys Comp. 614 (2014) 353–359.
[7] X.Q. Fu, J.Y. Liu, Y.T. Wan, X.M. Zhang, F.L. Meng, J.H. Liu, Preparation of a leaf-like CdS micro-/nanostructure and its enhanced gas-sensing properties for detecting volatile organic compounds, J. Mater. Chem. 22 (2012) 17782–17791.
[8] Z. Skoufa, E. Heracleous, A.A. Lemonidou, On ethane ODH mechanism and nature of active sites over NiO-based catalysts via isotopic labeling and methanol sorption studies, J. Catal. 322 (2015) 118–129.
[9] Y.Z. Zheng, H.Y. Ding, M.I. Zhang, Preparation and electrochemical properties of nickel oxide as a supercapacitor electrode material, Mater. Res. Bull. 44 (2009) 403–407.
[10] X.Y. Yan, X.L. Tong, J. Wang, C.W. Gong, M.G. Zhang, L.P. Liang, Hydrothermal-synthesized NiO nanowall array for lithium ion batteries, J. Alloys Comp. 556 (2013) 56–61.
[11] S. Lv, C.G. Wang, S.X. Xing, Hexamethylenetetramine-induced synthesis of hierarchical NiO nanostructures on nickel foam and their electrochemical properties, J. Alloys Comp. 603 (2014) 190–196.
[12] H.J. Kim, J.H. Lee, Highly sensitive and selective gas sensors using p-type oxide semiconductors: overview, Sens. Actuators B 192 (2014) 607–627.
[13] B. Miao, W. Zeng, L.Y. Lin, S. Xu, Characterization and gas-sensing properties of NiO nanowires prepared through hydrothermal method, Physica E 52 (2013) 40–45.
[14] J.H. Lee, Gas sensors using hierarchical and hollow oxide nanostructures: overview, Sens. Actuators B 140 (2009) 319–336.
[15] M.Y. Wu, W. Zeng, Y.Q. Li, Hydrothermal synthesis of novel SnO_2 nanoflowers and their gas-sensing properties, Mater. Lett. 104 (2013) 34–36.
[16] C. Wang, R.Z. Sun, X. Li, Y.F. Sun, P. Sun, F.M. Liu, G.Y. Lu, Hierarchical flower-like WO_3 nanostructures and their gas sensing properties, Sens. Actuators B 204 (2014) 224–230.
[17] F.L. Meng, N.N. Hou, S. Ge, B. Sun, Z. Jin, W. Shen, L.T. Kong, Z. Guo, Y.F. Sun, H. Wu, C. Wang, M.Q. Li, Flower-like hierarchical structures consisting of porous single-crystalline ZnO nanosheets and their gas sensing properties to volatile organic compounds (VOCs), J. Alloys Comp. 626 (2015) 124–130.
[18] Q. Li, Y.J. Chen, T. Yang, D.N. Lei, G.H. Zhang, L. Mei, L.B. Chen, Q.H. Li, T.H. Wang, Preparation of 3D flower-like NiO hierarchical architectures and their electrochemical properties in lithium-ion batteries, Electrochim. Acta 90 (2013) 80–89.
[19] X. Cao, Y.J. Xu, N. Wang, Facile synthesis of NiO nanoflowers and their electrocatalytic performance, Sens. Actuators B 153 (2011) 434–438.
[20] L.X. Yang, Y.J. Zhu, H. Tong, Z.H. Liang, W.W. Wang, Hierarchical α-Ni$(OH)_2$ and NiO carnations assembled from nanosheet building blocks, Cryst. Growth Des. 7 (2007) 2716–2719.
[21] H.M. Du, L.F. Jiao, K.Z. Cao, Y.J. Wang, H.T. Yuan, Polyol-mediated synthesis of mesoporous α-Ni$(OH)_2$ with enhanced supercapacitance, Appl. Mater. Interfaces 5 (2013) 6643–6648.
[22] Y. Cai, J.M. Ma, T.H. Wang, Hydrothermal synthesis of α-Ni$(OH)_2$ and its conversion to NiO with electrochemical properties, J. Alloys Comp. 582 (2014) 328–333.
[23] L.P. Zhu, G.H. Liao, Y. Yang, H.M. Xiao, J.F. Wang, S.Y. Fu, Self-assembled 3D flower-like hierarchical β-Ni$(OH)_2$ hollow architectures and their in situ thermal conversion to NiO, Nanoscale Res. Lett. 4 (2009) 550–557.
[24] A.G. Al-Sehemi, A.S. Al-Shihri, A. Kalam, G. Du, T. Ahmad, Microwave synthesis, optical properties and surface area studies of NiO nanoparticles, J. Mol. Struct. 1058 (2014) 56–61.
[25] A.D. Tang, X.Y. Li, Z. Zhou, O.Y. Jing, H.M. Yang, Mechanochemical synthesis of Ni$(OH)_2$ and the decomposition to NiO nanoparticles: thermodynamic and optical spectra, J. Alloys Comp. 600 (2014) 204–209.
[26] A. Chrissanthopoulos, S. Baskoutas, N. Bouropoulos, V. Dracopoulos, P. Poulopoulos, S.N. Yannopoulos, Synthesis and characterization of ZnO/NiO

p–n heterojunctions: ZnO nanorods grown on NiO thin film by thermal evaporation, Photon. Nanostruct. – Fundamentals Appl. 9 (2011) 132–139.
[27] M. Alagiri, S. Ponnusamy, C. Muthamizhchelvan, Synthesis and characterization of NiO nanoparticles by sol–gel method, J. Mater. Sci.: Mater. Electron. 23 (2012) 728–732.
[28] N. Barsan, U. Weimar, Conduction model of metal oxide gas sensors, J. Electroceram. 7 (2001) 143–167.
[29] N.M. Shaalan, T. Yamazaki, T. Kikuta, Influence of morphology and structure geometry on NO_2 gas-sensing characteristics of SnO_2 nanostructures synthesized via a thermal evaporation method, Sens. Actuators B 153 (2011) 11–16.
[30] C. Balamurugan, A.R. Maheswari, D.W. Lee, Structural, optical, and selective ethanol sensing properties of p-type semiconducting $CoNb_2O_6$ nanopowder, Sens. Actuators B 205 (2014) 289–297.
[31] N. Barsan, C. Simion, T. Heine, S. Pokhrel, U. Weimar, Modeling of sensing and transduction for p-type semiconducting metal oxide based sensors, J. Electroceram. 25 (2010) 11–19.
[32] S. Pokhrel, C.E. Simion, V. Quemener, N. Bârsan, U. Weimar, Investigations of conduction mechanism in Cr_2O_3 gas sensing thick films by ac impedance spectroscopy and work function changes measurements, Sens. Actuators B 133 (2008) 78–83.